Available online at www.sciencedirect.com
ScienceDirect
Trans. Nonferrous Met. Soc. China 26(2016) 1736−1744
Transactions of Nonferrous Metals Society of China
www.tnmsc.cn

Effect of processing route on grain refinement in pure copper processed by equal channel angular extrusion

Chao-lan TANG[1], Hao LI[2], Sai-yi LI[3,4]

1. School of Electro-Mechanical Engineering, Guangdong University of Technology, Guangzhou 510006, China;
2. Guangdong Institute of Special Equipment Inspection and Research, Zhongshan 528400, China;
3. School of Materials Science and Engineering, Central South University, Changsha 410083, China;
4. Key Laboratory of Nonferrous Metal Materials Science and Engineering, Ministry of Education, Central South University, Changsha 410083, China

Received 29 July 2015; accepted 18 November 2015

Abstract: An experimental study of the microstructures in pure copper billets processed by 8 passes of equal channel angular extrusion (ECAE) via an extended range of processing routes with a 90° die is carried out. Each processing route is defined according to the inter-pass billet rotation angle (χ), which varies from 0° to 180°. According to the generation of high-angle boundaries and reduction of grain size by electron backscatter diffraction (EBSD) measurements, the grain refinement is found to be most efficient for route with χ=90° and least efficient with χ=180°, among the seven routes studied. This trend is supported by supplementary transmission electron microscopy (TEM) measurements. Comparison of the EBSD and TEM data reveals the importance of considering the non-equiaxity of grain structures in quantitative assessment of microstructural differences in ECAE-processed materials.

Key words: pure copper; equal channel angular extrusion; severe plastic deformation; strain path; grain refinement

1 Introduction

Severe plastic deformation (SPD) has been developed as a promising approach to obtain ultrafine-grained (UFG) metallic materials [1]. Among various SPD techniques, equal channel angular extrusion (ECAE) [2] is unique in its viability of controlling strain path change (SPC), which is known to have significant influence on the deformation behavior of grains. A large range of SPCs can be introduced by changing the "processing route" [1,3], which is defined by an optional rotation (χ) about the billet longitudinal axis between successive passes (see Fig. 1). While the effects of other processing parameters (e.g., die angle and number of passes) on grain refinement have been well demonstrated in the literature, and that of the processing route remained to be a subject under debate for more than a decade [3−13]. To date, most of the experimental studies have been devoted to face-centered cubic (FCC) metals processed via three basic routes, designated as *A* (χ=0°), *B* (χ=90°) and *C* (χ=180°). Route *B* (also known as B_C, see Ref. [1]) has often been considered to be the most effective in producing equiaxed grains. However, contradictory views exist about the optimal route for grain refinement, especially for materials processed using 90° dies. The discrepancies between different studies are sometimes attributed to different methods and parameters used in microstructure characterization (see e.g., Refs. [14,15]).

Most interpretations of the dependency of grain refinement on processing route are based on macroscopic deformation features, such as shear band interaction [2], alignment of macroscopic shear plane [6,7], and redundancy of plastic strain [5]. Due to the lack of consideration of necessary physics related to the grain deformation, these theories showed limited successes. BEYERLEIN et al [8] attempted to sort the grain refinement efficiencies of the basic routes by following the number of shape-based grain splits during crystal

Foundation item: Project (50871040) supported by the National Natural Science Foundation of China; Project (NCET-06-0741) supported by the Program for New Century Excellent Talents of China
Corresponding author: Sai-yi LI; Tel: +86-731-88876621; E-mail: saiyi@csu.edu.cn
DOI: 10.1016/S1003-6326(16)64286-3

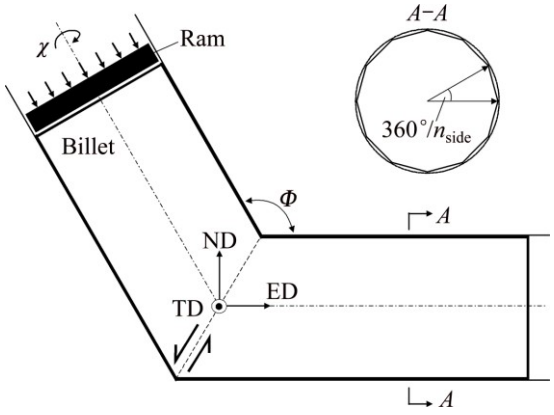

Fig. 1 Schematic of die geometry in ECAE and optional billet rotation (χ) between successive passes defining processing route (Inset illustrates the shape of the channels' cross-section, n_{side} denotes the number of sides of the polygon [13]; ED, ND and TD stand for extrusion, normal and transverse directions, respectively)

plasticity simulations that explicitly accounted for deformation mechanisms. Alternatively, LI et al [11] analyzed the mesomechanical behavior in ECAE by crystal plasticity simulations. It was shown that the slip activities in transitional periods between successive passes vary significantly with the processing route and that a higher fraction of newly activated slip systems might promote a higher efficiency of grain refinement. This theory has been partly validated with preliminary results obtained for pure Cu [11] and pure Al [13].

In the present study, the microstructure development in multi-pass ECAE of pure Cu processed via extended processing routes was studied experimentally. The results obtained demonstrate the significance of route design in ECAE processing. Compared with the earlier assessment in Ref. [11], the present study highlights the consistency of grain refinement between different microstructure characterization methods. The importance of considering the non-equiaxity of microstructures is discussed.

2 Experimental

The material considered in this work was a 12 mm-thick hot-rolled commercially pure Cu (C11000) plate. As shown by the optical micrographs taken from the normal plane of the as-received plate (Fig. 2), the material consisted of equiaxed grains with an average grain size of about 60 μm. Billets with 65 mm in length were machined from the as-received Cu plate with the longitudinal direction of the billet parallel to the rolling direction of the plate. The billets were subjected to ECAE at room temperature for 8 passes via 7 different routes using a Φ=90° die with an outer corner angle of Ψ=16°, at a ram speed of 3.3 mm/s. These routes are designated hereafter as E0, E45, E75, E90, E105, E135 and E180, respectively, wherein the character 'E' signifies ED (i.e., the axis around which the rotation is carried out after each pass) and the number stands for the value of χ (in degree). χ is counter-clockwise positive from the right view of the outlet channel. Accordingly, routes E0, E90 and E180 are equivalent respectively to the basic routes *A*, *B* and *C* generally considered in the literature. To prevent unintended billet rotations about its longitudinal axis during its passage through the channels, these experiments were conducted using special dies [16], in which the cross-sections of channels were 24-sided (i.e., n_{side}=24, see Fig. 1) regular polygons circumscribed in circles having a diameter of 10.0 mm for the inlet channel and 9.8 mm for the outlet channel. Similarly, the shape of the billet cross-section was a regular 24-gon with a 9.8 mm-diameter circumcircle. The billet and die channels were well lubricated with MoS_2-containing grease prior to each pass. The effective plastic strain (ε_e) accumulated after 8 passes is estimated to be 8.6, according to the formula of IWAHASHI et al [17].

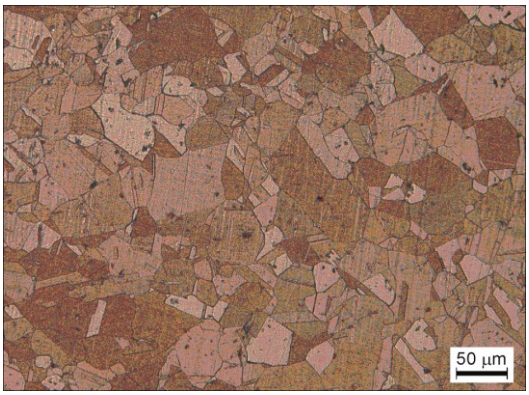

Fig. 2 Optical microstructure of as-received pure Cu plate

The microstructures in the ECAE-processed billets were characterized by electron backscatter diffraction (EBSD). The specimens were sectioned from the middle portion of each deformed billet by electro-discharge machining (EDM), with the plane surface normal to the TD. They were then prepared using standard metallographic preparation techniques with a final electro-polishing carried out in a 50/50 (volume ratio) orthophosphoric/de-ionized water mixture at a temperature of about −20 °C for about 10 s. The EBSD scans were conducted using a TSL OIM system on a FEI Sirion 200 field emission scanning electron microscope at an accelerating voltage of 20 kV. An area of 15 μm (ED) × 10 μm (ND) was measured for each sample with a step size of 0.05 μm. The orientation data were subjected to cleaning-up using the OIM analysis software, utilizing the "grain dilation" option with a grain tolerance angle of 5° and a minimum grain size of 2 points to remove single point with misorientations (θ)

greater than 5° from all neighboring points and "artificial grains" with less than 2 points, respectively. From the cleaned data, statistic microstructure parameters including grain size, misorientation, and grain shape aspect ratio (short to long axes of an ellipse fitted to the grain) were derived. The grain sizes were measured using the linear intercept method, parallel to ND and ED, respectively, for each sample. In assessment of misorientation angle distributions, a low misorientation cut-off of 2° was used to minimize misorientation noise.

For samples processed via selected processing routes, additional microstructure characterizations were conducted using transmission electron microscopy (TEM). Multiple specimens with a thickness of 0.5 mm were sliced from the middle portion of each billet with the normal of the specimen plane parallel to TD, by EDM. Disks with a diameter of 3 mm were then punched from these slices. Thin foil specimens were prepared by twin-jet electro-polishing the disks in a solution of 25/25/50 (volume ratio) orthophosphoric acid/ethanol/ distilled water at a temperature of about 20 °C and a voltage of about 10 V. The observations were carried out on a Hitachi H−800 TEM at an accelerating voltage of 200 kV. Bright field micrographs and selected area diffraction (SAD) patterns with an aperture diameter of 2.3 μm were taken.

3 Results and discussion

3.1 EBSD observations

Figure 3 shows the EBSD grain maps of the Cu billets processed for 8 passes via 7 routes. High-angle boundaries (HABs) having misorientation angles >15° and low-angle boundaries (LABs) having misorientation angles between 2°−15° are indicated by black and grey lines, respectively. The color in the maps indicates the inverse pole figure (IPF) of TD. It is evident that, compared to that of the initial material, the microstructures after ECAE are significantly refined. They are generally characterized by a mixture of elongated grains and equiaxed grains. The presence of a significant amount of LABs indicates that many regions in these samples comprise subgrains. Notably, the microstructures developed via different routes depict noticeable differences in the grain size, boundary misorientation, and grain shape. For routes E0, E45, E135 and E180 (Figs. 3(a), (b), (f) and (g)), the samples show relatively large grains elongated along directions at small angles (~10°−25°) to the ED and there are very few equiaxed grains. With route E75 (Fig. 3(c)), the deformation structure is featured by elongated grains, but the grains are considerably refiner than those of the other routes stated above. With routes E90 and E105 (Figs. 3(d) and (e)), the structures are mainly composed of equiaxed submicron grains, though a small number of elongated large grains exist in some local regions. It is also worthwhile to note from the IPFs that the textures developed after ECAE via different processing routes show considerable differences. A detailed evaluation of this aspect has been presented in previous work based on X-ray diffraction measurements [16].

Figure 4 summarizes the variations of grain size, fraction of HABs and grain shape with the processing route. The average grain size is shown by the mean intercept length measured along the ND and ED, respectively. The grain shape is represented by the aspect ratio, i.e., the length ratio of short to long axes. Evidently, the mean intercept length is smaller along the ND than that along ED, regardless of the route (Fig. 4(a)). This is consistent with the grain morphology shown in Fig. 3, as the grains are generally elongated at small angles with respect to the ED. It appears from Figs. 4(a) and (b) that route E90 is most efficient in both reduction of grain size and generation of HABs. The next most efficient route is E75 in terms of HAB generation or E105 in terms of grain size reduction. Meanwhile, the least efficient route is found to be E180, followed by E0. The average grain size obtained from the least efficient route is about two times that of the most efficient one, and the fraction of HABs obtained from the least efficient route is only about half of that of the most efficient one. These results demonstrate a clear influence of the processing route on the grain refinement efficiency, as briefly noted in an earlier assessment [11]. It is also interesting to further note from Fig. 4(c) that route E90 is actually the route that leads to the mostly equiaxed grain structure among all routes considered. The advantage of using route E90 in generating equiaxed grain structures has been successfully interpreted by considering intersections of the macroscopic shear planes [7].

Figures 5 and 6 show the grain size (ND intercept length) and misorientation angle distributions, respectively, in samples processed via the seven processing routes. It appears from these results that the basic characteristics in the grain size or misorientation distribution are similar for the samples processed via different processing routes. The basic features in the distributions observed for the present Cu are similar to those reported for commercial purity Al and pure Cu in Refs. [15,18,19]. The effect of processing route can be mainly seen in the variation of details in the distributions with the processing route. For samples processed via routes E0, E45 or E180, a relatively broad distribution of grain size with the maximum grain size up to ~3 μm is found. Comparatively, the other routes lead to narrower distributions with the largest grains less than ~2 μm in size. Figure 6 reveals that sample processed via route E90 depicts a considerably higher fraction of high-angled

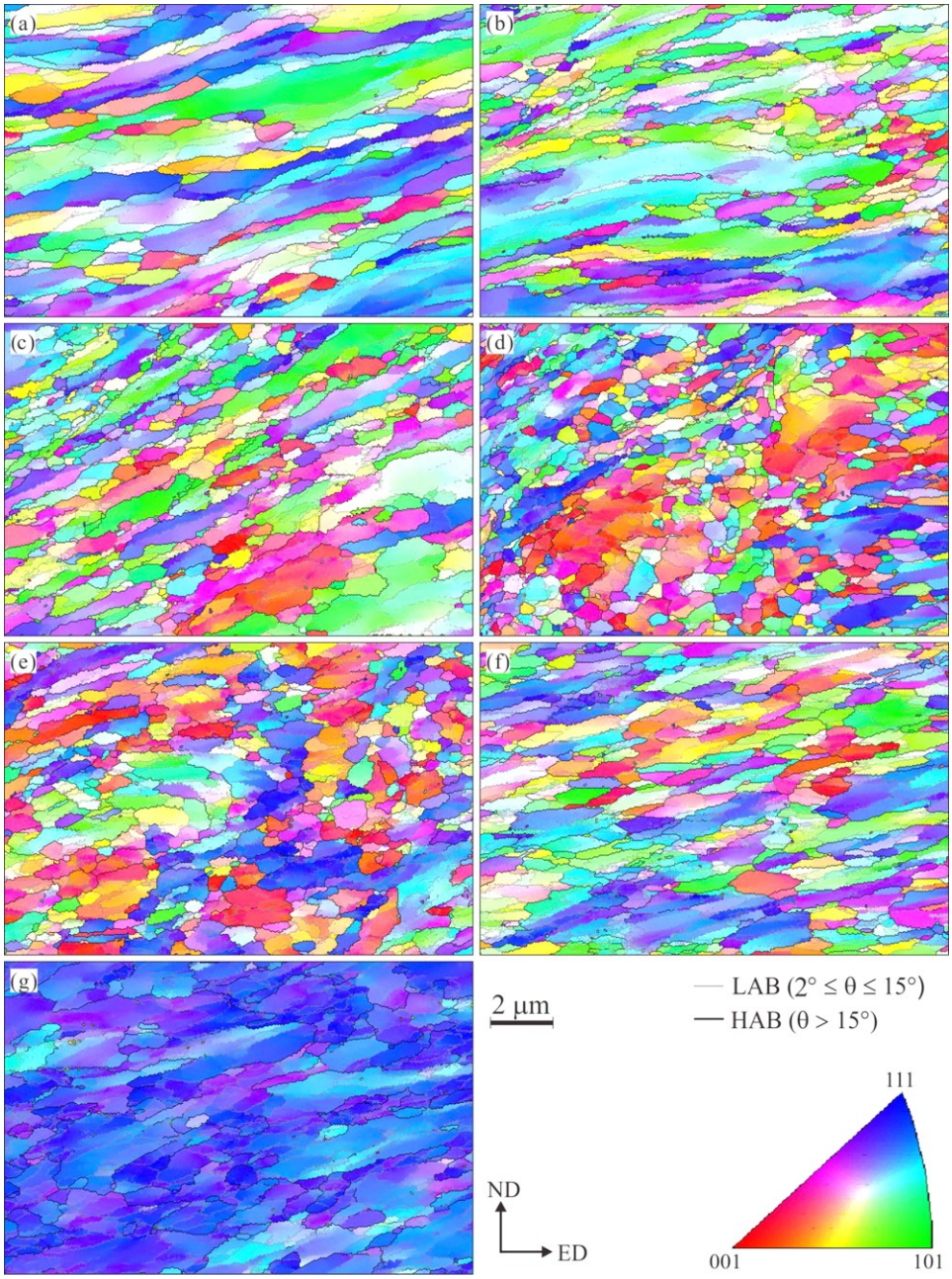

Fig. 3 EBSD grain maps of Cu samples processed by 8 passes of ECAE passes via different routes: (a) E0; (b) E45; (c) E75; (d) E90; (e) E105; (f) E135; (g) E180

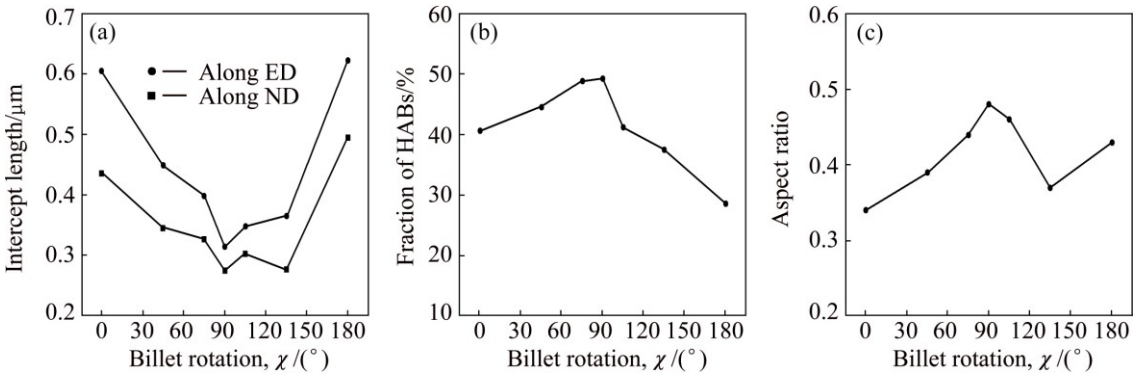

Fig. 4 Variations of statistic microstructure parameters with processing route in Cu samples processed by 8 passes of ECAE: (a) Intercept length; (b) Fraction of HABs; (c) Grain aspect ratio

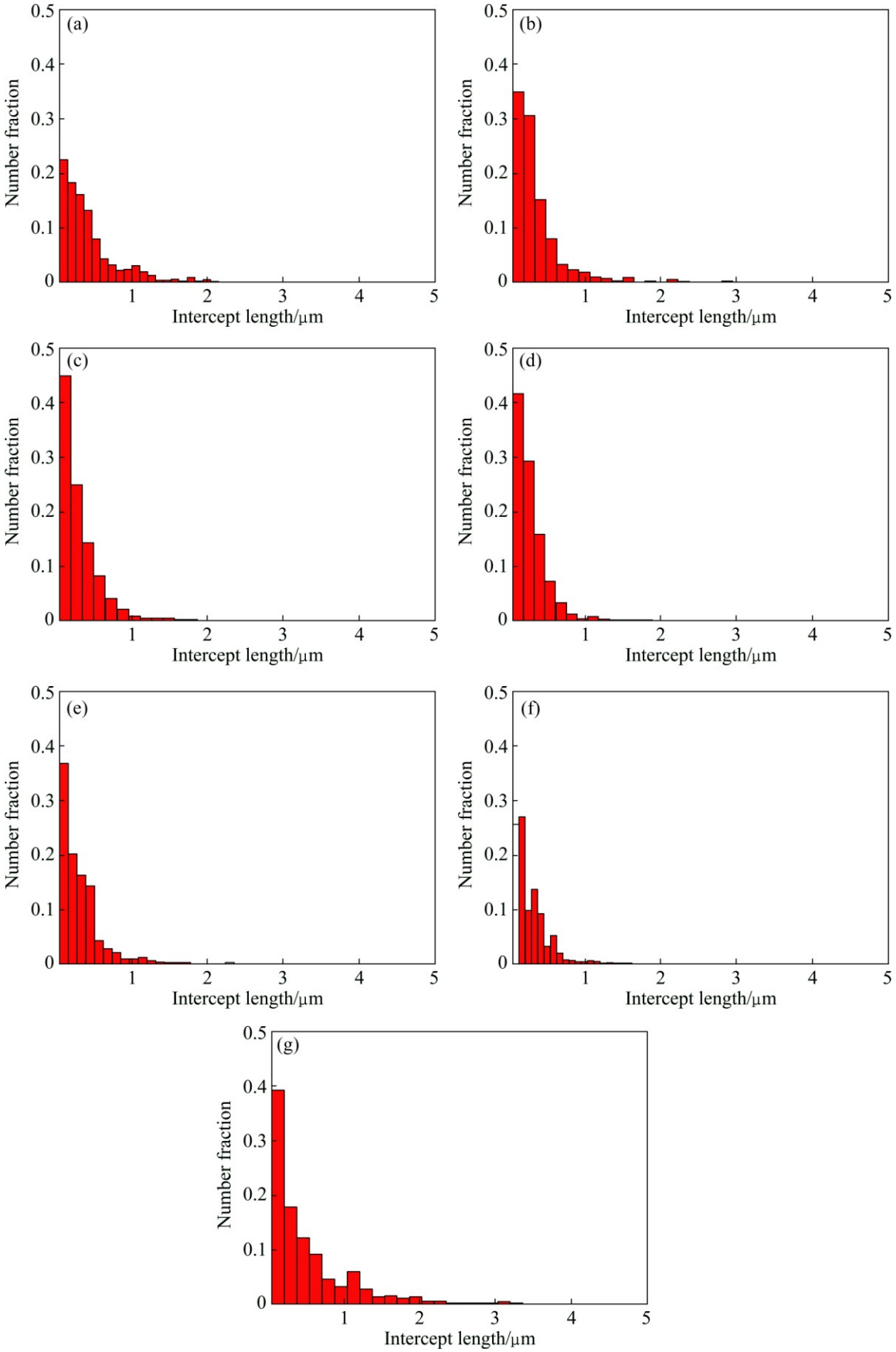

Fig. 5 Grain size (ND intercept length) distributions in Cu samples processed by 8 passes of ECAE via different routes: (a) E0; (b) E45; (c) E75; (d) E90; (e) E105; (f) E135; (g) E180

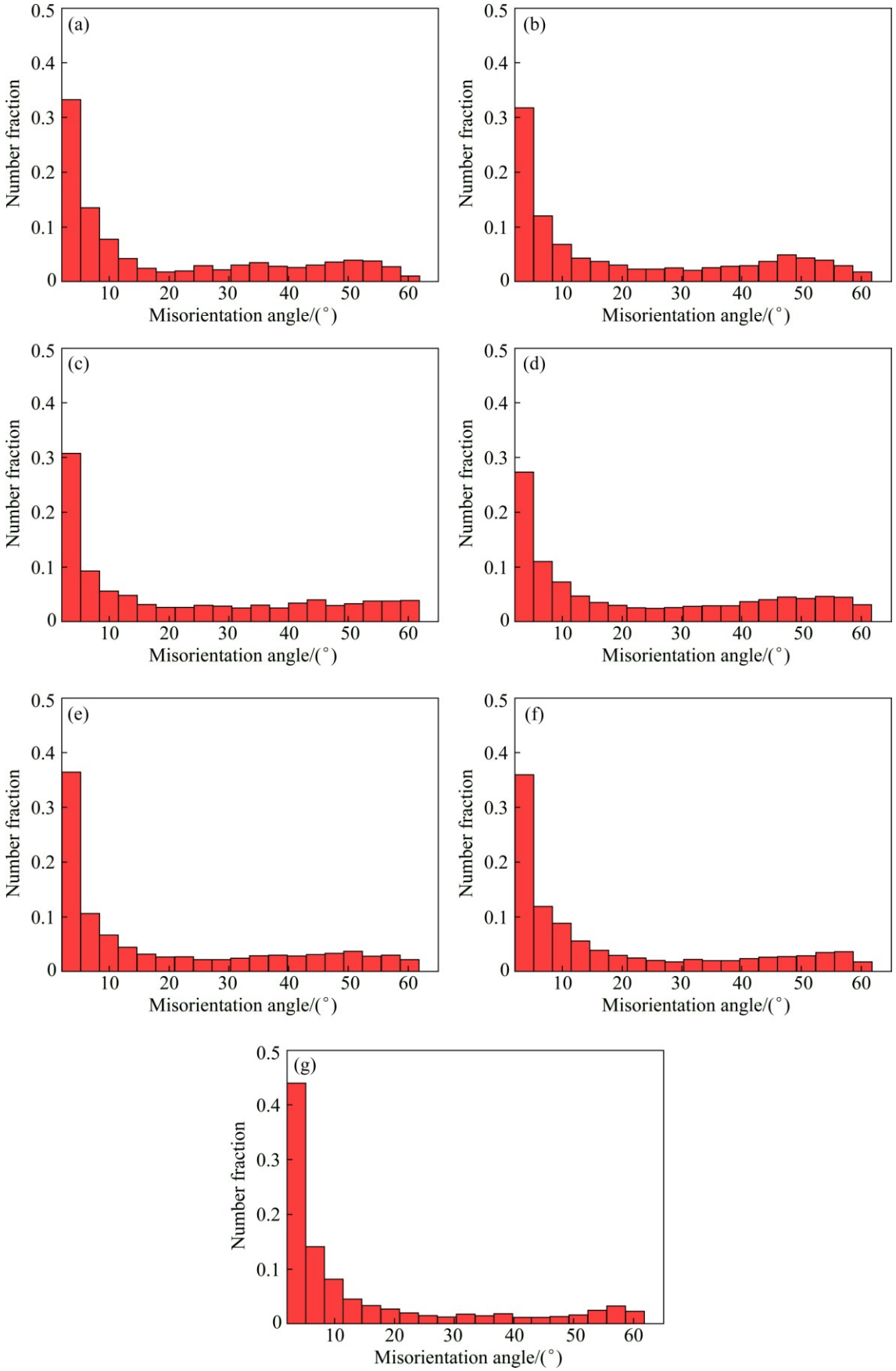

Fig. 6 Misorientation angle distributions in Cu samples processed by 8 passes of ECAE via different routes: (a) E0; (b) E45; (c) E75; (d) E90; (e) E105; (f) E135; (g) E180

misorientations than that of route E180. For other routes, the misorientation distributions show features that are intermediate between the two basic routes stated above. Overall, these results are consistent with the grain refinement efficiency shown by the average values in Fig. 4.

3.2 TEM observations

Figure 7 presents representative TEM images and the corresponding SAD patterns taken from the TD-plane of Cu samples processed for 8 passes of ECAE via routes E0, E90 and E180, respectively. These results confirm that for all samples, the microstructure in the material is significantly refined after ECAE. The samples generally consist of an UFG microstructure comprising extended lamellar boundaries (LBs), which are similar to dense dislocation walls [20]. The interior of a lamella is often composed of several dislocation cells, which are arranged approximately normal to the LBs and have low dislocation density in the interior. Therefore, the microstructure in these samples can be described as a mixture of elongated lamellae and nearly-equiaxed subgrains, though none of these routes leads to fully equiaxed structures. Despite these common features, there are considerable differences in the microstructures of samples processed via different routes. The microstructure generated with route E90 (Fig. 7(b)) is considerably finer than those of routes E0 and E180, while the latter two seem to result in a similar level of grain refinement. Meanwhile, the SADs of these samples show slightly more diffused patterns in the sample processed via route E90 than routes E0 and then E180. This means that boundary misorientation angles in the sample processed via route E90 are larger than those of routes E0 and then E180. Nonetheless, most boundaries are of low-angled configuration, irrespective of processing route.

For a quantitative assessment of the grain refinement, Fig. 8 shows the average cell sizes measured for the Cu billets processed via the three routes. These measurements were conducted manually using the intercept length method along two directions, approximately parallel and perpendicular to the LBs, respectively. To increase statistical reliability, four to five micrographs were measured for each sample. The broad statistical spread of data points (as indicated by the error bars in the figures) indicates considerable microstructure heterogeneity at the TEM length scale. Two interesting observations can be noted from these results. Firstly, for each sample, the cell size measured parallel to the LBs is considerably larger than that normal to the LBs. The differences between these two measurements are similar to those of the intercept lengths measured along the two perpendicular directions from the EBSD maps (see Fig. 4(a)), and both reflect the actual aspect ratio of the cells or subgrains. Similar differences have been noted for ECAE-processed Cu by DALLA TORRE et al [21]. Secondly, the cell sizes estimated from the TEM micrographs are comparable to, though slightly smaller than, the (sub)grain sizes measured by EBSD. Importantly, the cell sizes measured along the two directions seem to indicate different trends in the effect of processing route. According to the cell size parallel to the LBs, the microstructure is more refined via route E90 than that via routes E180 and then E0, in reasonable agreement with the trend shown by the EBSD results (see Fig. 4(a)). However, the effect of processing route becomes negligible when the cell sizes normal to the LBs are considered. These results suggest that it is necessary to consider sufficiently the non-equiaxity of the grain

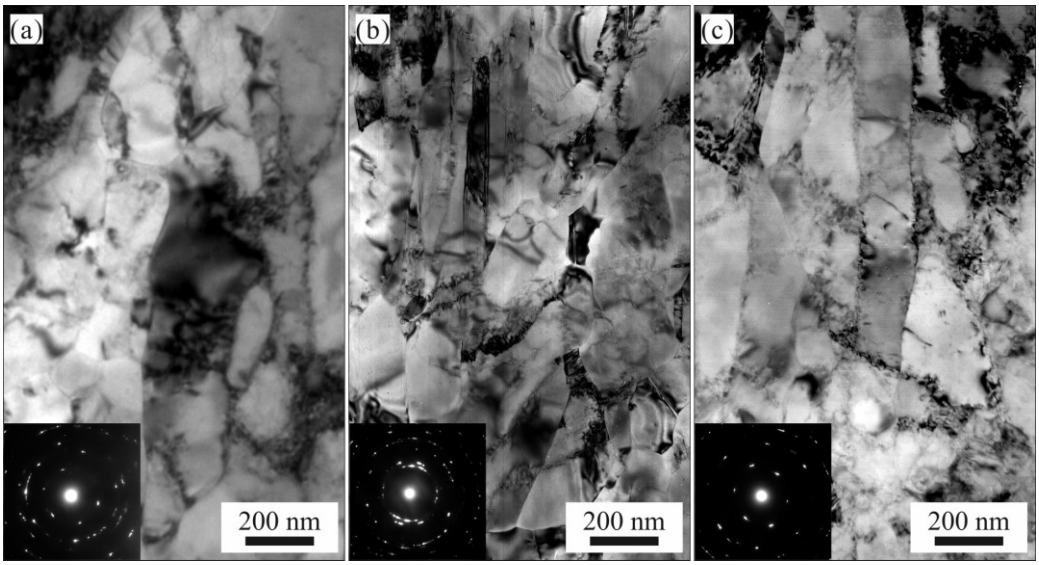

Fig. 7 TEM images taken on TD-section of Cu samples processed by 8 passes of ECAE via different routes: (a) E0; (b) E90; (c) E180

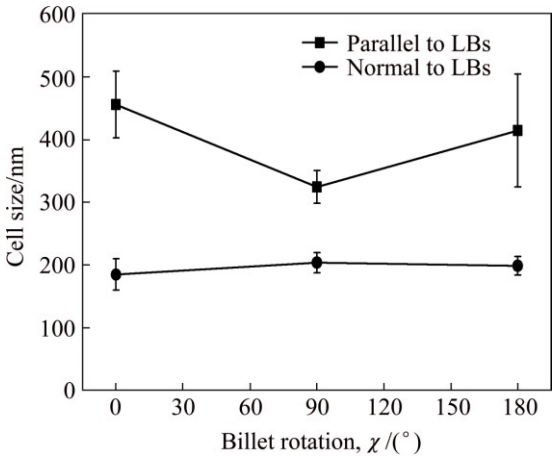

Fig. 8 Variation of cell size with processing route in Cu samples processed by 8 passes of ECAE

structures in detailed comparison of microstructure differences. Compared with TEM, EBSD measurements seem to provide a more consistent and statistically reliable evaluation of the dependency of grain refinement on processing route.

3.3 Comparison of experiments with theoretical expectations

The present experiments have demonstrated that the pure Cu material can be significantly refined by ECAE to 8 passes. The size of the substructures developed in the deformed samples is reduced to submicron level. With the EBSD measurements, the grain sizes (i.e., intercept length) measured along two perpendicular directions indicate similar trends in the effect of processing route on grain size reduction. These trends, combined with the effect of processing route on misorientation development, suggest that routes E90 and E180 are respectively the most and least efficient routes for grain refinement. These findings are supported by supplementary TEM observations, as along as the non-equiaxity of the microstructures is reasonably considered in the analysis.

In the literature, previous experimental observations in FCC metals processed by ECAE with 90° die do not reveal a consistent trend of the relative grain refinement efficiency, even for the three basic routes. For the pure Cu in the present experiments, the relative efficiency of these routes can be sorted in a descending order as E90 > E0 > E180. This order of efficiency coincides with that found in the literatures in some cases [19], but contradicts some others [15,22], and all of these studies in the literature used pure Al or Al alloys (see details in Ref. [11]). As noted in the introduction, existing theories based solely on macroscopic deformation are insufficient to explain such processing route-dependencies of grain refinement. Instead, recent polycrystal plasticity simulations suggested that the variation of grain refinement efficiency with processing route in ECAE could be well correlated to the significance of newly activated slip systems at the pass-to-pass transitions [11]. Accordingly, the grain refinement efficiency in ECAE with the 90° die was anticipated to be the highest via route E75 and the lowest via route E180, among the processing routes examined at an interval of χ of 15° [11]. The experimental trend found for the present Cu samples with the aid of EBSD and TEM observations is broadly consistent with this prediction.

4 Conclusions

1) The EBSD measurements of the ECAE-processed pure Cu reveal substantial variations of the microstructure development with the processing route in a relatively large range of processing routes, confirming the significance of route design in producing UFG materials.

2) Due to the non-equiaxity of the microstructures generated by ECAE, sufficient care should be taken in quantitative assessment of the microstructures. Compared with TEM, EBSD measurements provide a more statistically reliable evaluation of the dependency of grain refinement on processing route.

3) In consideration of both the generation of HABs and grain size reduction, the grain refinement in the Cu samples is found to be most efficient with route E90 and least efficient with route E180. This trend can be reasonably explained by the slip activity based theory in the literature.

Acknowledgments

CT is grateful to Ms. N. QIN for the help with the EBSD data analysis during her visiting stay at Central South University, China. Thanks are due to Mr. X. LI for the help with the EBSD sample preparation and measurements.

References

[1] VALIEV R Z, LANGDON T G. Principles of equal-channel angular pressing as a processing tool for grain refinement [J]. Progress in Materials Science, 2006, 51: 881−981.

[2] SEGAL V M. Equal channel angular extrusion: From macromechanics to structure formation [J]. Materials Science and Engineering A, 1999, 271: 322−333.

[3] DUPUY L, RAUCH E F. Deformation paths related to equal channel angular extrusion [J]. Materials Science and Engineering A, 2002, 337: 241−247.

[4] IWAHASHI Y, HORITA Z, NEMOTO M, LANGDON T G. The process of grain refinement in equal-channel angular pressing [J]. Acta Materialia, 1998, 46: 3317−3331.

[5] GHOLINIA A, PRANGNELL P B, MARKUSHEV M V. The effect of strain path on the development of deformation structures in severely deformed aluminium alloys processed by ECAE [J]. Acta

Materialia, 2000, 48: 1115−1130.
[6] ZHU Y T, LOWE T C. Observations and issues on mechanisms of grain refinement during ECAP process [J]. Materials Science and Engineering A, 2000, 291: 46−53.
[7] FURUKAWA M, HORITA Z, LANGDON T G. Factors influencing the shearing patterns in equal-channel angular pressing [J]. Materials Science and Engineering A, 2002, 332: 97−109.
[8] BEYERLEIN I J, LEBENSOHN R A, TOME C N. Modeling texture and microstructural evolution in the equal channel angular extrusion process [J]. Materials Science and Engineering A, 2003, 345: 122−138.
[9] LI S, MISHIN O V. Analysis of crystallographic textures in aluminum plates processed by equal channel angular extrusion [J]. Metallurgical and Materials Transactions A, 2014, 45: 1689−1692.
[10] ROODPOSHTI P S, FARAHBAKHSH N, SARKAR A, MURTY K L. Microstructural approach to equal channel angular processing of commercially pure titanium—A review [J]. Transactions of Nonferrous Metals Society of China, 2015, 25: 1353−1366.
[11] LI S, LI X, YANG L. Role of strain path change in grain refinement by severe plastic deformation: A case study of equal channel angular extrusion [J]. Acta Materialia, 2013, 61: 4398–4413.
[12] LI Sai-yi. Application of crystal plasticity modeling in equal channel angular extrusion [J]. Transactions of Nonferrous Metals Society of China, 2013, 23: 170−179.
[13] LI S, ZHENG X, ZHANG M. Grain refinement in pure aluminum severely deformed by equal channel angular extrusion via extended processing routes [J]. Metallurgical and Materials Transactions A, 2014, 45: 2601−2611.
[14] SUN P L, KAO P W, CHANG C P. Effect of deformation route on microstructural development in aluminum processed by equal channel angular extrusion [J]. Metallurgical and Materials Transactions A, 2004, 35: 1359−1368.
[15] MISHIN O V, BOWEN J R, LATHABAI S. Quantification of microstructure refinement in aluminium deformed by equal channel angular extrusion: Route A vs. route Bc in a 90° die [J]. Scripta Materialia, 2010, 63: 20−23.
[16] LI S, LI H. Texture evolution in pure copper processed by equal channel angular extrusion with extended processing routes [J]. Materials Science Forum, 2011, 667−669: 271−276.
[17] IWAHASHI Y, WANG J, HORITA Z, NEMOTO M, LANGDON T G. Principle of equal-channel angular pressing for the processing of ultra-fine grained materials [J]. Scripta Materialia, 1996, 35: 143−146.
[18] MISHRA A, RICHARD V, GRÉGORI F, ASRARO R J, MEYERS M A. Microstructural evolution in copper processed by severe plastic deformation [J]. Materials Science and Engineering A, 2005, 410−411: 290−298.
[19] SALEM A A, LANGDON T G, MCNELLEY T R, KALIDINDI S R, SEMIATIN S L. Strain-path effects on the evolution of microstructure and texture during the severe-plastic deformation of aluminum [J]. Metallurgical and Materials Transactions A, 2006, 37: 2879−2891.
[20] HUGHES D A, HANSEN N. High angle boundaries formed by grain subdivision mechanisms [J]. Acta Materialia, 1997, 45: 3871−3886.
[21] DALLA TORRE F, LAPOVOK R, SANDLIN J, THOMSON P F, DAVIES C H J, PERELOMA E V. Microstructures and properties of copper processed by equal channel angular extrusion for 1−16 passes [J]. Acta Materialia, 2004, 52: 4819−4832.
[22] CABBIBO M. Use of TEM Kikuchi bands for microstructure and thermal stability study of ECA pressed AA1200 via routes A, C, Bc [J]. Reviews on Advanced Materials Science, 2010, 25: 113−121.

等通道转角挤压加工路径对纯铜晶粒细化的影响

唐超兰[1]，李 豪[2]，李赛毅[3,4]

1. 广东工业大学 机电工程学院，广州 510006；
2. 广东省特种设备检测研究院，中山 528400；
3. 中南大学 材料科学与工程学院，长沙 410083；
4. 中南大学 有色金属材料科学与工程教育部重点实验室，长沙 410083

摘 要：针对经过 90°模具、8 道次等通道转角挤压的纯铜，采用电子背散射电子衍射(EBSD)和透射电镜(TEM)分析大范围内加工路径对其显微组织演变的影响。每个路径按照道次间棒料绕其长轴转动角度(χ)进行定义，角度变化范围为 0°~180°。EBSD 所测大角度晶界比例和晶粒大小结果表明，当 χ=90°时晶粒细化效率最高，χ=180°时晶粒细化效率最低。该趋势得到 TEM 结果的进一步佐证。对比 EBSD 和 TEM 结果还发现，在定量比较 ECAE 材料的显微组织差异时，应该充分考虑晶粒组织形貌的非等轴特征。

关键词：纯铜；等通道转角挤压；剧烈塑性变形；应变路径；晶粒细化

(Edited by Wei-ping CHEN)